

Cardiac metastasis of neuroendocrine tumor of the thymus diagnosed by cardiac magnetic resonance T1 mapping: a case report

Journal of International Medical Research

48(6) 1–7

© The Author(s) 2020

Article reuse guidelines:

sagepub.com/journals-permissions

DOI: 10.1177/0300060520931678

journals.sagepub.com/home/imr



Jiamin Zhang and Mu Zeng 

Abstract

Carcinoid heart disease is a late complication of carcinoid syndrome, and imaging can help in the diagnosis of diffuse cardiac metastasis. We herein report a case of diffuse cardiac metastasis of a neuroendocrine tumor of the thymus diagnosed using different imaging modalities. Cardiac magnetic resonance imaging played an important role in the diagnosis. The patient underwent conservative medical treatment and remained able to perform his usual activities of daily living.

Keywords

Carcinoid heart disease, cardiac magnetic resonance imaging, cardiac metastasis, neuroendocrine tumor of the thymus, biopsy, case report

Date received: 7 November 2019; accepted: 13 May 2020

Introduction

Carcinoid heart disease is a late cardiac manifestation of neuroendocrine tumors of the thymus (NETTs), and T1 mapping may be useful in the diagnosis of diffuse cardiac metastasis. We herein report a case in which diffuse cardiac metastasis of an NETT was diagnosed with the help of a magnetic resonance imaging (MRI) technique. The diagnosis was confirmed by biopsy.

Department of Radiology, The Second Xiangya Hospital, Central South University, Changsha, Hunan 410011, China

Corresponding author:

Mu Zeng, Department of Radiology, The Second Xiangya Hospital, Central South University, No. 139 RenMin Zhong Lu, FuRong District, Changsha, Hunan Province 410011, China.

Email: zengmu@csu.edu.cn



Creative Commons Non Commercial CC BY-NC: This article is distributed under the terms of the Creative

Commons Attribution-NonCommercial 4.0 License (<https://creativecommons.org/licenses/by-nc/4.0/>) which permits non-commercial use, reproduction and distribution of the work without further permission provided the original work is attributed as specified on the SAGE and Open Access pages (<https://us.sagepub.com/en-us/nam/open-access-at-sage>).

Case report

A 53-year-old man underwent an abdominal computed tomography (CT) scan because of generalized abdominal pain, and pericardial effusion was incidentally detected. The patient had recently developed a paroxysmal cough and expectoration without additional symptoms. For further evaluation, the patient was admitted to the Outpatient Department of Cardiology. Upon admission, he was in good spirits with a body temperature of 36.4°C, heart rate of 80 bpm, and blood pressure of 135/66 mmHg. Physical examination revealed no palpable lymphadenopathy and no jugular venous distension. The trachea was positioned along the midline, and the thyroid was normal in size. The bilateral lung sounds were clear, without dry or wet rales. The heart was enlarged, the heart rate was regular, S1 and S4 were reduced, and a stage 3/6 systolic murmur was heard in the fourth intercostal space of the left margin of the sternum.

An electrocardiogram demonstrated left ventricular hypertrophy, T-wave inversion in many leads, and poor R-wave progression in leads V1 to V3. Laboratory examination revealed a creatine kinase level of 42.2 U/L (reference, 18.0–198.0 U/L), N-terminal pro-B-type natriuretic peptide level of 9511.33 pg/mL (reference,

<300 pg/mL), and troponin T level of $8.77 \times 10^3 \mu\text{g/L}$ (reference, <0.1 $\mu\text{g/L}$).

Echocardiography showed left ventricular wall thickening; mild reflux of the mitral, tricuspid, pulmonary, and aortic valves; left ventricular diastolic dysfunction; and pericardial effusion. These findings were compatible with hypertrophic cardiomyopathy. The patient was sent for cardiac MRI (CMR) and chest CT in our hospital. Chest CT showed an anterior superior mediastinal mass of about 7×6 cm that was inhomogeneous after enhancement and involved the left pulmonary vein; mediastinal lymph node enlargement was also observed. A puncture biopsy of the mediastinum was performed.

CMR showed asymmetrical thickening of the left ventricular wall, diastolic dysfunction of the left ventricle, and pericardial effusion (Figure 1). T1-weighted imaging demonstrated diffuse thickening of the left ventricular myocardium with nodular change, and no evidence of myocardial edema was seen on T2 fat suppression. Cine images showed normal systolic function with an ejection fraction of 51%, diastolic dysfunction, and a slight increase in the volume of pericardial effusion (Figure 2). Myocardial perfusion imaging showed multiple left ventricular nodular perfusion defects without delayed enhancement, while the remainder of the

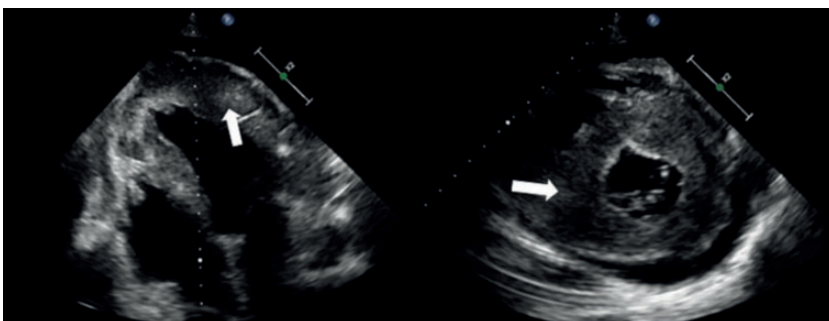


Figure 1. Echocardiography of the four cardiac chambers (left) and short-axis view (right). The left ventricular wall is markedly thickened (arrows).

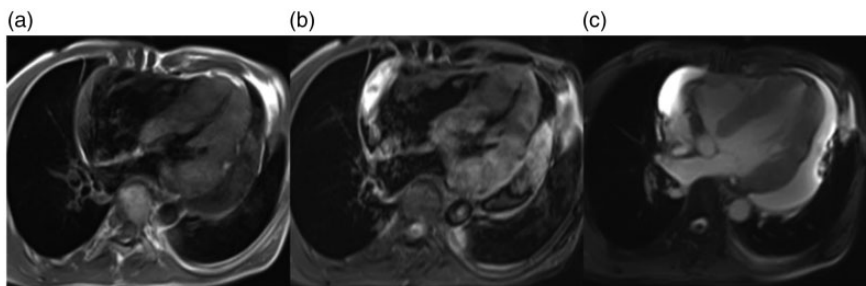


Figure 2. (a) T1-weighted magnetic resonance image showed a nodular left ventricular wall with a uniform signal. (b) T2 fat-suppression magnetic resonance image showed no clear myocardial edema. (c) Cine image showed normal systolic function with an ejection fraction of 51% and large volume.

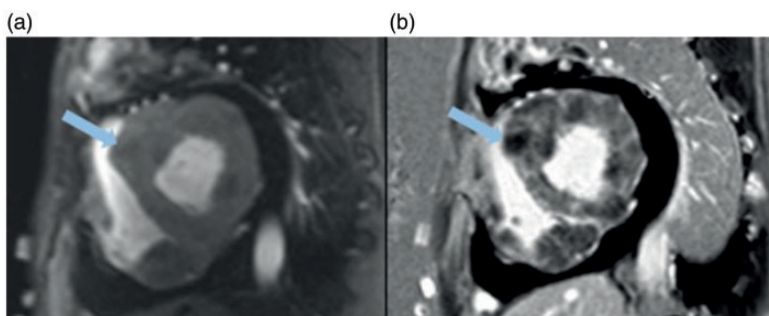


Figure 3. (a) Myocardial perfusion images showed nodular perfusion defects in the left ventricular septum (arrow). (b) Delayed enhancement showed that the perfusion defect area had no obvious enhancement and that the rest of the myocardium was non-uniformly enhanced.

myocardium was diffusely enhanced on delayed imaging (Figure 3). T1 mapping revealed an abnormal signal of the left ventricular wall. The native T1 time of the myocardium was increased beyond 1500 ms, which is significantly higher than that of the normal myocardium (approximately 1109 ms¹), allowing for visualization of masses. The native T1 time of the metastatic area was slightly lower than that of the necrotic area. However, on post-contrast T1 mapping, the post-T1 time of the metastatic area was significantly lower than that of the necrotic area (Figure 4). Chest CT showed an irregular soft tissue density in the anterior mediastinum with non-uniform enhancement, low-density necrotic

foci, and ectatic vasculature (Figure 5). A core biopsy of the anterior mediastinum confirmed a neuroendocrine tumor (typical type) (Figure 6). For treatment, levocarnitine was used to improve the myocardial metabolism and prevent heart failure, and metoprolol was used to protect the heart. Because of the marked increase in the B-type natriuretic peptide level, furosemide and spironolactone were added to improve cardiac function, and a licorice compound mixture was used to relieve coughing and phlegm production. For economic reasons, the patient refused surgical treatment and asked to be discharged from the hospital. After 6 months of follow-up, the patient's activities of daily living were

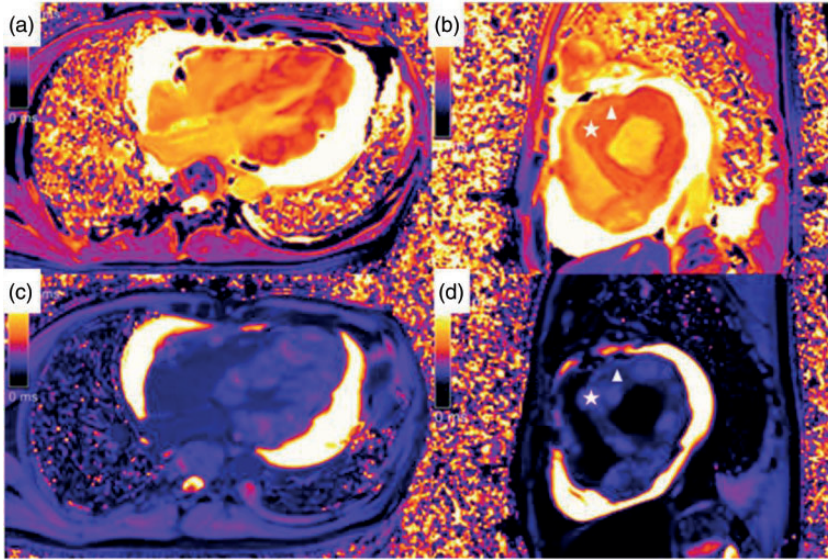


Figure 4. (a, b) Pre-contrast T1 map of the four cardiac chambers and the short-axis view. The native T1 value of the necrotic area was 1551 ms, and that of the metastatic area was 1502 ms. Both were significantly higher than the T1 values in the normal myocardium. (c, d) Post-contrast T1 map of the four chambers and short-axis view. The post-T1 value of the necrotic area was 844 ms, and that of the metastatic area was 602 ms. The T1 value of the transferred tissue was lower than that of the necrotic tissue, allowing it to be identified.

slightly restricted, but the restriction was acceptable.

Informed consent was obtained from the patient for the publication of this case report. The study protocol was approved by the Ethics Committee of the Second Xiangya Hospital, Central South University.

Discussion

The T1 mapping technique, also known as the longitudinal relaxation time quantitative imaging technique, is based on inversion or saturation pulse train acquisition. In most cases, CMR T1 mapping is performed by balanced steady-state free precession. After excitation with the recovery pulse of inversion (or saturation), the MRI signal is collected many times after a series of reversal times (or saturation times), and the T1 recovery curve is then calculated by

the corresponding function to obtain the value of T1. Our patient was examined in the supine position using a 3.0T scanner (Skyra; Siemens Medical Solutions, Erlangen, Germany). A steady-state free precession sequence was used to collect left ventricular two-chamber, four-chamber, and short-axis movie images at the end of inhalation. The parameters were a repetition time of 42.38 ms, echo time of 1.43 ms, flip angle of 44°, field of view of 320 × 400 mm, matrix of 126 × 224, left ventricle short-axis slice thickness of 8 mm, and acquisition of 8 to 10 layers. One study showed that native T1 values were significantly longer in patients with hypertrophic cardiomyopathy than in healthy controls [1373 ms (1312–1452 ms) vs. 1279 ms (1229–1326 ms); $P < 0.0001$].¹⁰ Another study showed that myocardial T1 was significantly elevated in patients with cardiac amyloidosis than in normal subjects and patients with

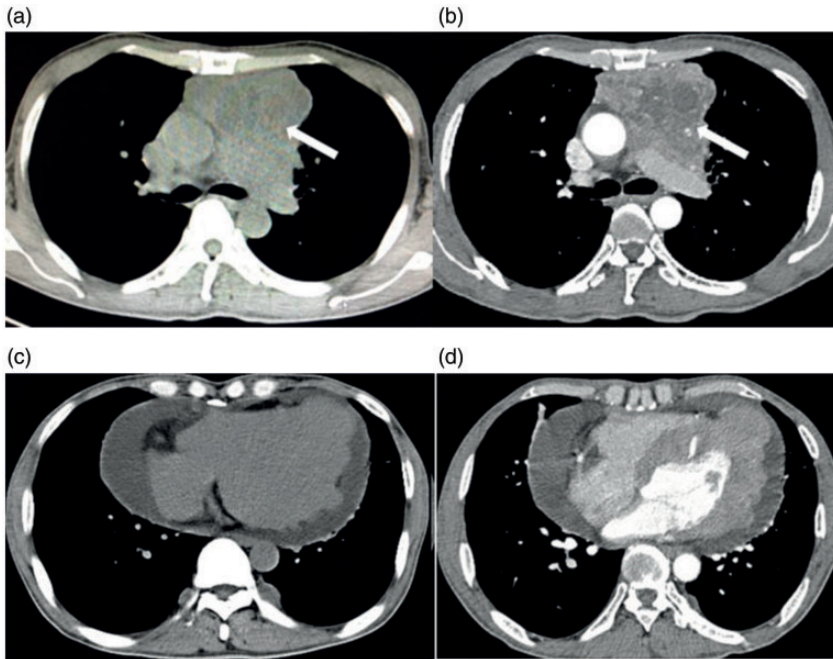


Figure 5. (a) Chest computed tomography showed an irregular soft tissue density in the anterior mediastinum. (b) Contrast-enhanced chest computed tomography showed non-uniform enhancement of the mass, with low-density necrotic foci and chaotic blood vessels. (c) Unenhanced and (d) enhanced computed tomography slices of the cardiac ventricle.

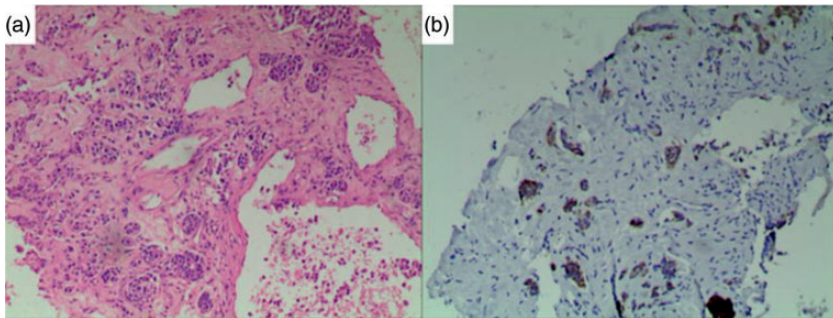


Figure 6. (a) Small numbers of heterogeneous cells in a proliferating fibrous tissue were observed by hematoxylin and eosin staining (original magnification, $\times 100$). (b) Immunohistochemical staining revealed CK(+), Vim(+), Ki-67 (5%+), CD5(-), TDT(-), S100(+), HMB45(-), LCA(-), MC(-), CR(-), TTF-1(-), MyoD1(-), myogenin(-), PSA(-), P504s(-), CK5/6(-), CD56(-), Syn(+), CK7(-), and CgA(+) (CgA, Syn, Ki-67, and CK are commonly used in the diagnosis of neuroendocrine tumors).

hypertrophic cardiomyopathy (1497.3 ± 22.0 ms vs. 1273.3 ± 30.1 and 1329.3 ± 42.6 ms, both $P < 0.05$).¹¹ Edema, fibrosis,

and inflammation increase the T1 value; in contrast, lipid accumulation, bleeding, and iron overloading can decrease the T1 value.

Our patient presented with paroxysmal cough and expectoration, without specific symptoms related to heart disease. MRI demonstrated that the T1 time of the left ventricular wall calculated by the quantitative T1 mapping technique was abnormal. The post-T1 time of the myocardium was significantly different, allowing us to easily distinguish between different organizational characteristics.

Primary NETTs are exceedingly rare tumors, constituting about 0.4% of all carcinoid tumors² and less than 5% of all anterior mediastinal tumors.³ According to the 2015 World Health Organization tumor classification, NETTs are classified into four histological types: typical and atypical carcinoids (well-differentiated neuroendocrine carcinomas) and small- and large-cell neuroendocrine carcinomas (poorly differentiated neuroendocrine carcinomas).⁴ NETTs are usually characterized by a local mass and nonspecific symptoms. Because of their insidious onset, clinical symptoms and signs lack specificity and the diagnosis is evasive.

Unlike neuroendocrine tumors growing in the gastroenteropancreatic tract, NETTs show very aggressive biological behavior. Araki et al.⁸ reported that NETTs present as large, lobulated, heterogeneous masses with an infiltrative nature. Metastasis and recurrence are frequent. The liver, brain, and bone are the most common sites of metastasis of this tumor. However, metastasis to the heart is rare.⁵ Farooqui et al.⁶ reported cardiac metastasis of a carcinoid neoplasm in the right ventricle, which was a solid and isolated mass connected with the interventricular septum. In addition, Gaur et al.⁹ reported that an advanced tumor stage is correlated with poorer long-term survival ($P=0.009$) and that clinical outcomes are better in patients who undergo surgery than in patients who do not ($P=0.005$). The authors found no

survival benefit for radiation delivered as a part of primary therapy.⁹ In the present case, the cardiac metastases exhibited invasive growth and a diffuse distribution, and echocardiography showed asymmetrical thickening of the left ventricular wall and diastolic dysfunction; therefore, the diagnosis of hypertrophic cardiomyopathy was made. T1- and T2-weighted MRI could not detect the tumor metastasis because of lack of contrast; however, T1 mapping could quantitatively measure the T1 values of the myocardium, allowing for the detection of diffuse lesions. Thus, we were able to differentiate tumor infiltration from necrosis by measuring the myocardial T1 value. Metastasis is characterized by a significant increase in T1 with areas of liquefaction and necrosis. In patients with hypertrophic cardiomyopathy, focal myocardial fibrosis can occur in the presence of normal myocardium, which can be distinguished by the T1 value, without obvious liquefactive necrosis. Amyloidosis is characterized by diffuse deposition of amyloid in the myocardium, a diffuse increase in T1, and no obvious liquefaction necrosis.

Carcinoid heart disease is a late complication of carcinoid syndrome. Carcinoid tumors may result in a constellation of symptoms that are termed carcinoid syndrome (e.g., secretory diarrhea and episodic cutaneous flushing). These symptoms are caused by the release of vasoactive mediators and serotonin by the tumor into the systemic circulation. They may be described as a burning sensation and can be accompanied by tachycardia, palpitations, and dizziness caused by hypotension. Circulating serotonin induces widespread fibrosis of the valve and endocardium, which can cause valve regurgitation and cardiac dysfunction. The right heart is most often affected, and the left heart is spared in most cases because of hormone inactivation during transit through the

pulmonary vasculature. In a large study of carcinoid heart disease, 90% of patients had tricuspid regurgitation, 81% had pulmonary valve regurgitation, and 53% had pulmonary stenosis, causing right ventricular dysfunction and pulmonary hypertension. However, only 7% had left-sided valve involvement.⁷

Conclusion

We have described a patient with diffuse cardiac metastasis of an NETT. The typical MRI findings in such cases are a diffuse high native T1 time and different post-T1 time. Imaging in this case also revealed that the mediastinal mass produced hematogenous metastasis rather than direct invasion. These imaging findings may help in the diagnosis of diffuse cardiac metastasis.


Declaration of conflicting interest

The authors declare that there is no conflict of interest.

Funding

This work was supported by the National Natural Science Foundation of China (Grant Nos. 81701660 and 81671671).

ORCID iD

Mu Zeng  <https://orcid.org/0000-0002-2904-8193>

References

- Roy C, Slimani A, De Meester C, et al. Age and sex corrected normal reference values of T1, T2 T2* and ECV in healthy subjects at 3T CMR. *J Cardiovasc Magn Reson* 2017; 19: 72.
- Yao JC, Hassan M, Phan A, et al. One hundred years after “carcinoid”: epidemiology of and prognostic factors for neuroendocrine tumors in 35,825 cases in the United States. *J Clin Oncol* 2008; 26: 3063–3072.
- Filosso PL, Ruffini E, Solidoro P, et al. Neuroendocrine tumors of the thymus. *J Thorac Dis* 2017; 9: S1484–S1490.
- Marx A, Chan JK, Coindre JM, et al. The 2015 World Health Organization Classification of Tumors of the Thymus: continuity and changes. *J Thorac Oncol* 2015; 10: 1383–1395.
- Pandya UH, Pellikka PA, Enriquez-Sarano M, et al. Metastatic carcinoid tumor to the heart: echocardiographic-pathologic study of 11 patients. *J Am Coll Cardiol* 2002; 40: 1328–1332.
- Farooqui M, Rathore S and Ball T. Utility of indium-111 octreotide to identify a cardiac metastasis of a carcinoid neoplasm. *Proc (Bayl Univ Med Cent)* 2016; 29: 76–78.
- Saraf K, Tingi E, Brodison A, et al. A rare case of primary ovarian carcinoid. *Gynecol Endocrinol* 2017; 33: 766–769.
- Araki T, Sholl LM, Hatabu H, et al. Radiological features and metastatic patterns of thymic neuroendocrine tumours. *Clin Radiol* 2018; 73: 479–484.
- Gaur P, Leary C, Yao JC, et al. Thymic neuroendocrine tumors: a SEER Database analysis of 160 patients. *Ann Surg* 2010; 251: 1117–1121.
- Ogawa R, Kido T, Nakamura M, et al. T1 mapping using saturation recovery single-shot acquisition at 3-tesla magnetic resonance imaging in hypertrophic cardiomyopathy: comparison to late gadolinium enhancement. *Jpn J Radiol* 2017; 35: 116–125. DOI: 10.1007/s11604-017-0611-5.
- Cui Q, Yu J and Shen W. [Late gadolinium enhancement and T1 mapping for the diagnosis of cardiac amyloidosis]. *Zhonghua Wei Zhong Bing Ji Jiu Yi Xue* 2019; 31: 1538–1541. DOI: 10.3760/cma.j.issn.2095-4352.2019.12.021.